

## PROCEEDINGS B

**Making teeth to order: conserved genes reveal an ancient molecular pattern in paddlefish (*Actinopterygii*)**

Journal:	<i>Proceedings B</i>
Manuscript ID:	RSPB-2014-2700.R1
Article Type:	Research
Date Submitted by the Author:	22-Jan-2015
Complete List of Authors:	Meredith Smith, Moya; KCI Dental institute , Craniofacial Development Johanson, Zerina; Natural History Museum, Earth Sciences Butts, Thomas; King's College London, MRC centre for developmental neurobiology Ericsson, Rolf; Natural History Museum, Earth Sciences Modrell, Melinda; University of Cambridge, Physiology, Development and Neuroscience Tulenko, Frank; Kennesaw State University, Biology and Physics Davis, Marcus; Kennesaw State University, Biology and Physics Fraser, Gareth; University of Sheffield, Animal and Plant Sciences
Subject:	Developmental biology < BIOLOGY, Evolution < BIOLOGY, Genetics < BIOLOGY
Keywords:	Polyodon , teeth, dentition, shh, bmp4, paddlefish
Proceedings B category:	Evolutionary Biology

SCHOLARONE™  
Manuscripts

1 **Making teeth to order: conserved genes reveal an ancient molecular pattern in**  
2 **paddlefish (Actinopterygii)**

3

4 Moya M. Smith<sup>a,b</sup>, Zerina Johanson<sup>b</sup>, Thomas Butts<sup>c</sup>, Rolf Ericsson<sup>b</sup>, Melinda Modrell<sup>d</sup>,  
5 Frank J. Tulenko<sup>e</sup>, Marcus C. Davis<sup>e</sup>, and Gareth J. Fraser<sup>f</sup>

6

7 *<sup>a</sup>King's College London Dental Institute, Craniofacial Development and Stem Cell*

8 *Biology, UK; <sup>b</sup>Department of Earth Sciences, Natural History Museum, London, UK;*

9 *<sup>c</sup>MRC Centre for Developmental Neurobiology, King's College London, UK;*

10 *<sup>d</sup>Department of Physiology, Development and Neuroscience, University of Cambridge,*

11 *UK; <sup>e</sup>Department of Biology and Physics, College of Science and Mathematics,*

12 *Kennesaw State University, Georgia, USA; <sup>f</sup>Department of Animal and Plant Sciences,*

13 *University of Sheffield, UK.*

14

15 Corresponding author M.M. Smith: [moya.smith@kcl.ac.uk](mailto:moya.smith@kcl.ac.uk)

16

17 **Summary**

18 Ray-finned fishes (Actinopterygii) are the dominant vertebrate group today (+30,000

19 species, predominantly teleosts), with great morphological diversity, including their

20 dentitions. How dental morphological variation evolved is best addressed by

21 considering a range of taxa across actinopterygian phylogeny; here we examine the

22 dentition of *Polyodon spathula* (American paddlefish), assigned to the basal group

23 Acipenseriformes. Although teeth are present and functional in young individuals of

24 *Polyodon*, they are completely absent in adults. Our current understanding of

25 developmental genes operating in the dentition is primarily restricted to teleosts; we

26 show that *shh* and *bmp4*, as highly conserved epithelial and mesenchymal genes for  
27 gnathostome tooth development, are similarly expressed at *Polyodon* tooth loci, thus  
28 extending this conserved developmental pattern within the Actinopterygii. These genes  
29 map spatio-temporal tooth initiation in *Polyodon* larvae and provide new data in both  
30 oral and pharyngeal tooth sites. Variation in cellular intensity of *shh* maps timing of  
31 tooth morphogenesis, revealing a second odontogenic wave as alternate sites within  
32 tooth rows, a dental pattern also present in more derived actinopterygians.  
33 Developmental timing for each tooth field in *Polyodon* follows a gradient, from rostral  
34 to caudal and ventral to dorsal, repeated during subsequent loss of teeth. The transitory  
35 *Polyodon* dentition is modified by cessation of tooth addition, and loss. As such,  
36 *Polyodon* represents a basal actinopterygian model for the evolution of developmental  
37 novelty: initial conservation, followed by tooth loss, accommodating the adult trophic  
38 modification to filter-feeding.

39

#### 40 **Keywords**

41 *Polyodon*, teeth, dentition, *shh*, *bmp4*, Acipenseriformes, paddlefish, evolution

42

#### 43 **1. Introduction**

44 Most tooth development models reflect a bias toward morphologically derived  
45 vertebrates (e.g., zebrafish, mouse). However, more representative models for the  
46 evolution of developmental mechanisms of the dentition are provided by taxa at the  
47 base of extant vertebrate phylogenies. The basal actinopterygian Order  
48 Acipenseriformes includes fossil taxa as well as the American paddlefish *Polyodon*  
49 (Family Polyodontidae) and sturgeons (Family Acipenseridae, e.g. *Acipenser* [1, 2]) and  
50 represents an increasingly utilized system for addressing developmental questions in an

51 evolutionary context [3-6]. Due to their basal phylogenetic position, Acipenseriformes  
52 are a particularly relevant model to test hypotheses of tooth patterning and evolution.  
53 The dentition is lost in adult paddlefish and sturgeon, but present in younger  
54 individuals, although details of early stages of tooth development are poorly known [1-  
55 3, 7]. As pattern order for the forming dentition has previously been described for more  
56 derived actinopterygians, comparable data for *Polyodon* will provide significant  
57 information on mechanisms in more phylogenetically basal actinopterygians.

58         The secreted protein sonic hedgehog (*shh*) and the TGF- $\beta$  superfamily member  
59 bone morphogenetic protein4 (*bmp4*) are key dental patterning genes in vertebrates. *In*  
60 *situ* hybridisation assays demonstrate that the transcripts coding for *shh/bmp4* are  
61 present at the earliest sites of tooth initiation with focused, time specific loci of  
62 expression restricted to dental epithelium (*shh*) [8, 9] and co-expression in the  
63 underlying condensed mesenchyme (*bmp4*). Co-expression occurs on each  
64 oropharyngeal dentate field, from a diffuse band of dental competence (odontogenic  
65 band), to discrete placodes of single tooth initiation. Non-mammalian vertebrates for  
66 which this conserved pattern of *shh/bmp4* expression has been used to characterize  
67 dental patterning include a variety of teleosts (Osteichthyes, Actinopterygii): rainbow  
68 trout (*Onchorhynchus mykiss* [8, 9]), Mexican tetra (*Astyanax mexicanus* [10]),  
69 zebrafish (*Danio rerio* [11, 12]), several Lake Malawi cichlids [13], the freshwater  
70 pufferfish (*Monotretes abei* [14]), as well the Queensland lungfish (*Neoceratodus*  
71 *forsteri* [15]) and various snakes and lizards (Osteichthyes, Sarcopterygii, [16-18]) and  
72 the catshark *Scyliorhinus canicula* [19, 20]. As the only non-teleost actinopterygian yet  
73 surveyed, our new data from *Polyodon* will provide key phylogenetic support for the  
74 hypothesis that *shh* and *bmp4* are part of a conserved and ancient gene regulatory  
75 network for patterning vertebrate dentitions.

76 We predict that *Polyodon* will exhibit the conserved pattern of epithelial *shh*-  
77 positive loci, with comparable mesenchymal expression of *bmp4* [8], observed in other  
78 vertebrate taxa. Here we will use expression patterns for these genes, along with other  
79 histological and morphological datasets to demonstrate temporal differences in focal  
80 localization for each tooth site in *Polyodon*, mapping position and timing of tooth  
81 initiation to demonstrate how pattern order is established through co-ordinated gene  
82 activity. Our hypothesis is that this represents a basal condition of shared genetic  
83 regulation of tooth initiation times and topographic order for the Actinopterygii.

84

## 85 **2. Material and Methods**

### 86 **(a) Animal care and sacrifice**

87 Fertilized *Polyodon spathula* eggs were obtained from Osage Catfisheries, Inc. (Osage  
88 Beach, MO, USA) and raised to desired stages in recirculating, closed freshwater  
89 systems mimicking natural conditions (22°C, pH 7.2 ±0.7, salinity of 1.0 ± 0.2 p.p.t.  
90 [21]). *Polyodon* were euthanized in a lethal dose of MS-222 (Tricaine) and fixed for at  
91 least 24h (dependent of tissue volume) in 4% paraformaldehyde [21]. All animal care,  
92 feeding, and euthanization protocols were in accordance with an approved IACUC  
93 (Institutional Animal Care and Use Committee) Animal Care Protocol [KSU #12-001;  
94 NSF IOS 1144965].

### 95 **(b) Staging of larval *Polyodon***

96 *Polyodon* staging follows [3, 21]: lengths for individual specimens for stages 37-46, and  
97 other details of the staging, can be obtained from these. Feeding larvae (beyond stage  
98 46) are described as ‘days post-staging’ (dps) and juveniles by standard length (SL). At  
99 incubation temperature (22°C), the larval period between hatching (stage 36) and onset  
100 of exogenous feeding and yolk exhaustion (stage 46) proceeds at approximately one

101 stage per 24 hour period [21].

### 102 **(c) *in situ* hybridisation**

103 *In situ* hybridisation used standard protocols [5] with riboprobes for *shh* [22] or *bmp4*. *Bmp4*  
104 was cloned from cDNA using the forward primer CGA GGC TAC TTT GTT GCA CA and  
105 reverse primer TCC ACG TAC AGT TCG TGT CG. Selected whole larvae (stages 41-45)  
106 with *shh* or *bmp4* expression were embedded in 20% gelatin and vibratome-sectioned at  
107 50µm or, embedded in 30% sucrose, frozen in liquid nitrogen, and cryostat sectioned at 20µm.  
108 Numbers of specimens (antisense, comparable number of sense), *bmp* stages 34-39 n=7; 40-  
109 43 n=6; 44-46 n=6. *shh* stages 36 n=2; 38 n=3; 39 n=3; 40 n=2; 41 n=4; 42 n=2; 43 n=2; 45=  
110 6. Photomicrographs were taken with Zeiss Nomarsky optics, or an Olympus SZX16  
111 dissecting microscope equipped with a QImaging RetigaEXi digital camera.

### 112 **(d) Clearing and staining, CT-imaging**

113 Cleared and stained specimens (CS; Alizarin red and Alcian Blue [23]) were dissected  
114 and mounted as half-jaws. Older specimens were studied as CS skeletal preps under a  
115 stereomicroscope and CT-scanned (X-Tek HMX ST CT scanner, Image and Analysis  
116 Centre, Natural History Museum, London; MicroCT at Dental Institute, King's College  
117 London, GE Locus SP, creating volumes with voxel sizes 6.5µm) and rendered using  
118 the software program Drishti (<http://sf.anu.edu.au/Vizlab/drishti>).

### 119 **(e) Terminology**

120 The terms distal and proximal are used in the upper and lower jaws, with reference to  
121 the jaw joint (proximal) and symphysis (distal). The terms rostral and caudal, dorsal and  
122 ventral are used with respect to the body axes.

123

## 124 **3. Results**

125 In *Polyodon spathula* larvae, *shh* and *bmp4* expression reveal both the early events of

126 oral and pharyngeal dental patterning, and sequential addition of tooth loci as  
127 development proceeds. There are noticeable differences in the addition of new tooth  
128 germs in individual dentate fields, normally caudal, but exceptionally rostrally on the  
129 palatopterygoid tooth plate. Concerning timing along the body axis, tooth initiation  
130 begins in association with Meckel's cartilage, establishing a spatio-temporal gradient  
131 that extends from the oral, through to tooth sites in the pharyngeal cavities (figures 1, 2;  
132 electronic supplementary material, figure 4). Skeletal preparations provide additional  
133 data on pattern order; after tooth rows form on the dentary and dermopalatine, they  
134 develop on the more caudal palatopterygoids and first hypobranchials (figures 1*a*, *c*, 2*a*,  
135 *b*, respectively). Teeth are later organized into toothed plates, connected by basal bone  
136 of attachment, representing functional surfaces of the oropharyngeal dentition  
137 (electronic supplementary material, figure 2*c*; Table) [1-3].

138

139 **(a) Timing of *shh* expression in whole mounts maps sequential tooth initiation**  
140 **(stages 37-43)**

141 Spatial expression of *shh* occurs as focal loci, with changes in intensity coincident with  
142 each stage of tooth germ morphogenesis, mapping location and developmental timing  
143 for each tooth position (figures 1, 3, 4). This pattern of spatio-temporal expression  
144 identifies new tooth germs added relative to preexisting ones, in precise locations at  
145 sequential times, from one dentate region to another (electronic supplementary material,  
146 Table 1).

147 *Shh* expression is first observed in the odontogenic fields beginning at stage 37  
148 (figure 1*d*, electronic supplementary material, figure 4*b*). Strong expression loci on the  
149 odontogenic band occur first as focused placodes (stages 39-41; figures 1*a-e*), then  
150 expression as a cap around the cone of the tooth tip (figures 3*p*<sup>2</sup>, 4, electronic

151 supplementary material, figure 4c-h). These loci mark tooth positions within one row  
152 (figure 1; electronic supplementary material, figure 4i-p). *Shh* expression is next  
153 upregulated at alternate (second) tooth positions, within this same row (figure 1a-c, e,  
154 arrows). By stage 43 *shh* is downregulated in epithelial cells of older tooth germs  
155 around tooth cones. Accurate counts of tooth number from *shh* expression at these later  
156 stages relies on seeing tooth cones (using Nomarsky optics). Nevertheless, differences  
157 in total number between upper and lower jaws are observed (electronic supplementary  
158 material, Table 1); for example, at stages 40 and 42 there are more tooth loci on the  
159 dentary than dermopalatine (compare electronic supplementary material, figure 4g, h  
160 (new parasymphysial tooth on dentary) with 4e, f, and 4i-m (new loci added distally)  
161 with 4n).

162         Given this recognizable developmental sequence of epithelial *shh* expression,  
163 sites of tooth initiation can be identified along the rostrocaudal body axis. In both jaws  
164 at stages 39-40, there are four to five tooth buds in each dentary and dermopalatine  
165 field, contrasting with lack of tooth buds in more caudal toothed sites (electronic  
166 supplementary material, figure 4c-h). Later, at stage 41 the dentary and dermopalatine  
167 have seven tooth positions with alternating higher intensity of *shh* expression, and a  
168 new distal and proximal tooth germ, all in the same tooth row (figure 1e, i, arrows). As  
169 well, two *shh*-positive tooth loci are present on the first hypobranchial and the  
170 palatopterygoids (figure 1a-c, e, arrowheads). In stages 42-43 these *shh* expression sites  
171 are intense caps around the tooth cone (electronic supplementary material, figure 4la,  
172 lb), forming rings in later stages where *shh* is downregulated in cap cells (electronic  
173 supplementary material, figure 4o-p, further details see §3c, d, and figure 4).

174

175 **(b) *Bmp4* expression maps timing of co-operative activity during tooth**



176 **morphogenesis (stages 40-45, 1dps)**

177 All stages show *bmp4* expression associated with each tooth locus (figure 1*f-i*;  
178 electronic supplementary material, figure 5). When compared to stage-matched  
179 specimens stained for *shh*, intense expression of *bmp4* appears associated with  
180 mesenchyme of the newest forming tooth loci (figure 1*g, i*, arrows). Notably, stage 41  
181 and 45 *bmp4* expression shows upregulation in alternate positions of (second) tooth  
182 germs within the tooth row, on the dentary and dermopalatine, while the most rostral  
183 (first) tooth germs are dentine cones with *bmp4* downregulated in the papilla. Note these  
184 show strong papillary expression in more caudal sites, indicating that these are younger  
185 (figure 1*f, g, i*; asterisk versus arrows, respectively). However, on the palatopterygoid,  
186 the intense papillary *bmp4* expression of the younger loci is rostral to the dentine cones,  
187 as observed in the expression pattern for *shh* (i.e. an opposite second tooth addition  
188 pattern to the dentary and dermopalatine, electronic supplementary material, figure 5*h*’,  
189 st 42, 5*l*’, st 45, arrows

190 **(c) Cellular expression of *shh* during tooth germ morphogenesis, stage 45**

191 The exact location of expression within the epithelial tooth germ is shown in more detail  
192 in serial, parasagittal sections than in whole mount *in situs* (figure 3, electronic  
193 supplementary material, figure 4), while the mesenchyme of the dental papilla shows  
194 complimentary *bmp4* expression (electronic supplementary material, figure 6). Gene  
195 expression changes are associated with different tooth germ morphologies through  
196 development (figures 3*p*, 4), where different intensities are associated with specific  
197 timing of morphogenesis at each tooth site in the oropharyngeal cavity, including first  
198 locations of the sites on the branchial arches. These demonstrate a rostro-caudal  
199 activation gradient of tooth initiation for each dentate field. Initially, the placode shows  
200 intense *shh* and *bmp4* expression and is superficial (no dental lamina), with *shh* located

201 to the middle epithelial cells (figure 3*d, i, p*<sup>1</sup>). In the cap stage, *shh* is more intense in all  
202 epithelia, surrounding the papilla (figure 3*g, p*<sup>2</sup>; *bmp4*, electronic supplementary  
203 material, figure 6*b*). After dentine histogenesis, *shh* is downregulated in the cap cells but  
204 is strongly expressed in the epithelium as a collar around the tooth cone (cone+collar  
205 stage, figure 3*c, p*<sup>3</sup>). Subsequently, *shh* is downregulated around the whole tooth cone  
206 (figure 3*j, n, p*<sup>4</sup>), but within the adjacent dental epithelium (not the inner dental  
207 epithelium), *shh* is upregulated as an intense focal expression, attributed to an incipient,  
208 successive tooth germ (figures 3*j, n*; electronic supplementary material, figure 6*a, c, d*).  
209 In the second, alternate tooth position the same steps of *shh* expression are observed,  
210 including cap, and cone+collar stages (figure 3*f, h, k*).

211 Serial sections show these expression stages simultaneously throughout the  
212 oropharyngeal cavity. Loci of *shh* expression occur dorsally on the dermopalatine and  
213 palatopterygoid (figure 3*a-d, g*), and ventrally on the dentary and 1st hypobranchial (figure  
214 3*e, h, i*; electronic supplementary material, figure 6*a*), along with a focal spot on the  
215 infrapharyngobranchials dorsally and 1st and 2nd hypobranchials ventrally (figure 3*e, h, i*;  
216 electronic supplementary material, figure 6*a, d*), but a field of expression on the more caudal  
217 branchial arches (figure 3*e*). When dentine is present in the first dentary teeth, as a collar  
218 plus translucent cone, the more caudal, second tooth germ is only at the placode stage  
219 (figure 3*f*). In other sections, the first tooth appears as a translucent dentine cone with a  
220 second tooth at cap, or collar stage (figure 3*h*). All these observations show a staggered time  
221 difference in each second tooth germ, as well as the first (*bmp4* data, electronic  
222 supplementary material, figure 6*c, d*). Similar staggered stages are seen in the dermopalatine  
223 tooth germs, and those of the palatopterygoid relative to the dermopalatine (figure 3*m, n, g*).

224 The restriction of *shh* expression to an intense focal locus (placode) forms first  
225 in the evaginated epithelium above the cartilage on the 2nd, as in the 1st, hypobranchial

226 (figure 3*l*). The placode is superficial (i.e. forms without a dental lamina; figure 3*n*, *o*,  
227 3*p*<sup>1</sup>), but also evaginated at the cone-cap stages (figure 3*h*, 3*p*<sup>2</sup>), then just within the  
228 expanded dental epithelium at cone+collar stage (figure 3*k*, *n*, 3*p*<sup>3</sup>). When *shh* is  
229 downregulated in all dental epithelium around the tooth there is an upregulated intense  
230 locus of *shh* expression next to this first tooth, in the dental epithelium, ‘cone+bud’, not  
231 evaginated but located in the epithelium adjacent to the dentine cone. Papillae with taste  
232 buds on the inner oral epithelium always exhibit faint *shh* expression, similar in  
233 intensity to the downregulated collar epithelium (figures 3*o*, arrow, 4*c*, sensory papilla  
234 with differentiated cells), while *bmp4* expression is absent (electronic supplementary  
235 material, figure 6).

236

237 **(d) Skeletal preparations show tooth addition positions in 7dps larvae**

238 *i) Tooth development on upper jaw, dorsal branchial skeleton.* Tooth rows are present  
239 ventral to the upper jaw cartilage, both rostrally on the dermopalatine bone and caudally  
240 on the palatopterygoid. The dermopalatine has 17-20 ankylosed teeth, while the latter  
241 lacks an independent ossification at this stage, with teeth conjoined by the individual  
242 bone of attachment of each tooth (translucent rings, figure 2*a*, *c*, *g*, *h*). Caudal to the  
243 palatopterygoid are two paired patches of teeth, the first associated with the hyoid arch  
244 with six teeth, joined only by their bases (figure 2*c*, black arrow, white box, *k*). The  
245 second is associated with the 2nd infrapharyngobranchial, possessing four teeth (figure  
246 2*c*, white box, *j*). The dermopalatine bone represents the most developmentally  
247 advanced in the upper jaw with new unattached teeth being added caudal to tooth  
248 positions 2 and 4, as well as parasymphysially (arrows, figure 2*g*, *i*). On the ventral  
249 surface of the palatopterygoid cartilage the oldest teeth are joined together via  
250 attachment bone (dentine cones expanded into cylinders), with 11 teeth on the right

251 side, nine on the left. As opposed to the caudal tooth addition associated with the  
252 dermopalatine, two new teeth (lacking bony rings; figure 1g, h, arrows) are rostral to the  
253 attached (older) teeth.

254 *ii) Tooth development on lower jaw, ventral branchial skeleton.* Tooth rows are present  
255 dorsally on Meckel's cartilage, with 22 left and 21 right teeth fused to the dentary bone  
256 via bone of attachment with new, unattached teeth caudal to the attached (older) teeth  
257 and at proximal and distal ends of the row (Mc, figure 2d, e, arrows). Other toothed  
258 plates are caudal to Meckel's cartilage in the pharyngeal cavity, on the hypobranchials  
259 (first, 11 teeth; second, three teeth). Hypobranchial teeth are not ankylosed to bone but  
260 older teeth are joined at their bases via their individual bone of attachment (figure 2d, f,  
261 l). Three new teeth (not joined by bone of attachment) on left hypobranchial 1 are added  
262 caudally (figure 1f, arrows). By later functional stages, with increasing tooth numbers at  
263 all sites, pharyngeal teeth are arranged in radial rows (four to five teeth in each),  
264 differing from the oral dentition (electronic supplementary material, figure 2a, b).

265

## 266 **Discussion**

267 Combined data from ontogenetic stages of *Polyodon spathula* establishes sequences of  
268 gene expression and tooth morphogenesis in the oropharyngeal cavity, allowing  
269 spatiotemporal patterns of tooth initiation and development to be documented; tooth  
270 rows form on the dentary and dermopalatine before the more caudal palatopterygoids and  
271 first hypobranchials (figures 1a, c, 2a, b, respectively). Teeth are later organized into  
272 toothed plates, connected together by basal bone of attachment, independently of the  
273 membrane bone, representing early functional surfaces of the oropharyngeal dentition  
274 (electronic supplementary material, figure 2c). Skeletal whole mounts show where new  
275 teeth are added to individual dentate fields, while post-larval stages indicate that tooth

276 addition slows and teeth are lost (electronic supplementary material).

277         These observations indicate progressive rostral-caudal and ventro-dorsal tooth  
278 initiation/addition gradients within the oropharyngeal cavity: tooth addition occurs first  
279 on Meckel's cartilage, showing alternate patterns of gene expression along the tooth  
280 row, prior to the dermopalatine (stage 40, electronic supplementary material, figure 4g,  
281 *h*; stage 42, electronic supplementary material, figure 4*i-m* versus 4*n*). At 7dps, a larger  
282 number of teeth are present on the dentary (figure 2) and at later juvenile stages the  
283 dentary shows substantial toothless areas of membrane bone relative to other dentate  
284 regions in the oropharyngeal cavity, due to tooth related loss of attachment bone  
285 (electronic supplementary material, figures 1*f-i*, 3*c-f*, asterisk). With respect to a rostral-  
286 caudal gradient of tooth addition, the dentary and dermopalatine develop tooth germs  
287 with a cone of dentine before the palatopterygoid (electronic supplementary material,  
288 figure 5), while teeth in the oral cavity develop before those in the pharyngeal cavity.  
289 There is also a rostral-caudal progression in the pharyngeal cavity with the placode  
290 stage attained in hypobranchial 1, versus field expression on hypobranchials 2. The  
291 former has the most teeth; caudally hypobranchials 3 and 4 never show upregulated  
292 tooth loci. With respect to rostro-caudal tooth addition on each oral site, new tooth buds  
293 are initiated caudally on the dermopalatine and the dentary (figure 1*i*, electronic  
294 supplementary material, figure 5*m, n*), but new teeth form rostrally on the  
295 palatopterygoid (figure 2*g, h*).

296         Our results show that *shh* and *bmp4* expression data during *Polyodon* tooth  
297 initiation follows the same spatio-temporal order observed in all other non-mammalian  
298 vertebrate species assayed to date [8, 9, 14-17, 24]; however, our observations on the  
299 ordered sequence of timing of tooth germ initiation in oral and pharyngeal tooth sets  
300 also reveal directed rostro-caudal and ventro-dorsal patterns. This graded progression

301 has not previously been reported for actinopterygians, nor for gnathostome  
302 oropharyngeal dentitions. Nevertheless, tooth patterning, at least with respect to tooth  
303 initiation and differentiation appears evolutionarily stable and highly conserved among  
304 gnathostomes. For example, no differences in collocation of *shh* and *bmp4* expression  
305 were detected between developing oral and pharyngeal teeth in *Polyodon*, comparable  
306 to a variety of other taxa. Along with the ordered tooth initiation sequence, this implies  
307 that tooth germs in all regions are equivalent and conserved modular vertebrate units.

308         We have demonstrated cellular partitioning for *shh* and *bmp4* expression and  
309 sequential stages of tooth germ morphogenesis from ‘placode’, ‘cap’, ‘cone+collar’ to  
310 ‘cone +bud’ (figure 4). This is based on expression intensity that changes in a  
311 characteristic sequence within the dental epithelium, for each developing tooth germ.  
312 Notably, a new locus for strong expression forms alongside the developed, functional  
313 tooth (‘cone+bud’). We interpret this as the incipient tooth germ representing what we  
314 term a successional tooth. This is distinct from superficial, initial tooth ‘placodes’ and is  
315 consistent with observations that in actinopterygian fish, successional teeth form from  
316 the older tooth and not from a dental lamina [8]. In some actinopterygian taxa  
317 (Cyprinidae, derived teleosts), functional and replacement teeth can be retained as a  
318 pair, particularly during larval stages, although the functional tooth is eventually lost  
319 with the replacement tooth moving into place [25]. In *Polyodon*, by comparison, the  
320 functional tooth is retained and not lost in response to the presence of the successional  
321 tooth; the latter should therefore not be considered a replacement tooth *per se*. Tooth  
322 loss occurs much later in *Polyodon* in what appears to be a general reduction and loss in  
323 the oropharyngeal cavity. This suggests that the more typical osteichthyan dentition  
324 pattern, with tooth replacement, never happens and is altered at this early ontogenetic  
325 stage.

326 Despite the enormous diversity, the presence of teeth organized into a functional  
327 dentition is a shared feature among jawed vertebrates, undoubtedly one reason for their  
328 evolutionary success, allowing a variety of feeding niches to be exploited. This diversity  
329 is underpinned by a high degree of developmental genetic conservation, particularly in  
330 early development, in taxa such as trout [7, 8], cichlids [10, 24] and the pufferfish [12];  
331 these early patterns are also seen in sarcopterygian fish *Neoceratodus* [13] as well as the  
332 shark *Scyliorhinus* [17, 26]. This conservation is also present in the dentition of  
333 *Polyodon spathula*, with modifications early in development, including tooth retention  
334 and lack of replacement teeth. Tooth addition slows, while in *Acipenser*, teeth are lost,  
335 entirely linked to suction feeding adaptations [1, 2]. However, we currently lack  
336 information on candidate genes involved in tooth regeneration that may change, or be  
337 missing in *Polyodon* and *Acipenser* [7]; other basal taxa, such as *Polypterus*, show full  
338 dentitions with tooth replacement [27]. New analysis of genes directed towards key  
339 transitions from tooth initiation to replacement in *P. spathula* will offer insight into the  
340 evolution of tooth regeneration strategies and dental diversity. Modifications to the  
341 dentition that occur later in ontogeny, allow the diversity of vertebrate dentitions to be  
342 expressed [10], and are the precursor steps to the development of drastically different  
343 modes of feeding among the gnathostomes.

344

345 Acknowledgements.

346 We thank the Natural Environmental Research Council (NERC grants NE/K01434X1,  
347 NE/K014595/1, NE/K0122071/1) and National Science Foundation (IOS 1144965 to  
348 Davis) for financial support. We would like to thank the following curators for access to  
349 specimens in their collections: Oliver Crimmen and James MacLaine (NHM, London);  
350 Radford Arindell and Barbara Brown (AMNH). We would also like to thank Dan

351 Sykes, and Monique Welten (NHM), and Christopher Healy (KCL) for help with CT-  
352 scanning and James Massey (KSU) for help with *bmp4* specimen preparation.

353 Additionally, we thank the Kahrs family and Osage Beach Catfisheries for continued  
354 support of paddlefish research.

355

356 Data Accessibility.

357 Drishti files for scans of *Polyodon spathula* are available at

358 <http://chondrichthyes.myspecies.info/>.

359

360 References

361 1 Grande, L. and Bemis, W. E. 1991 Osteology and phylogenetic relationships of fossil  
362 and recent paddlefishes (Polyodontidae) with comments on the interrelationships  
363 of Acipenseriformes. *J. Vert. Paleo. Spec. Mem.* **1**, 1–121.

364 2 Bemis, W. E., Findeis, E. K., and Grande, L. 1997 An overview of Acipenseriformes.  
365 *Env. Biol. Fishes* **48**: 25–71.

366 3 Bemis, W. E. and Grande, L. 1992 Early development of the actinopterygian head. I.  
367 External development and staging of the paddlefish *Polyodon spathula*. *J. Morph.*  
368 **213**, 47–83.

369 4 Davis M. C. 2013 The deep homology of the autopod: Insights from Hox gene  
370 regulation. *Int. Comp. Biol.* **53**, 224–234. (DOI: 10.1093/icb/ict029).

371 5 Modrell, M. S., Buckley, D. and Baker, C. V. H. 2011a Molecular analysis of  
372 neurogenic placode development in a basal ray-finned fish. *Genesis* **49**, 278–  
373 294.

374 6 Modrell, M. S., Bemis, W. E., Northcutt, R. G., Davis, M. C. and Baker, C. V. H.

375 2011b Electrosensory ampullary organs are derived from lateral line placodes in



- 376 bony fishes. *Nature Comm.* **2** (496), 3142–3146. (DOI: 10.1038/ncomms1502).
- 377 7 Hilton, E. J., Grande, L. and Bemis, W. E. 2011 Skeletal anatomy of the shortnose  
378 sturgeon, *Acipenser brevirostrum* Lesueur 181, and the systematics of sturgeons  
379 (Acipenseriformes, Acipenseridae). *Fieldiana (Life Earth Sci.)* **3**, 1–168.
- 380 8 Fraser, G. J., Graham, A. and Smith, M. M. 2004 Conserved deployment of genes  
381 during odontogenesis across osteichthyans. *Proc. Biol. Sci.* **271**, 2311–2317.
- 382 9 Fraser, G. J., Berkovitz, B. K., Graham, A. and Smith, M. M. 2006 Gene deployment  
383 for tooth replacement in the rainbow trout (*Oncorhynchus mykiss*): a  
384 developmental model for evolution of the osteichthyan dentition. *Evol. Dev.* **8**,  
385 446–457.
- 386 10 Stock, D. W., Jackman, W. R. and Trapani, J. 2006 Developmental genetic  
387 mechanisms of evolutionary tooth loss in cypriniform fishes. *Development*, **133**,  
388 3127–3137.
- 389 11 Jackman, W. R., Yoo, J. J. and Stock, D. W. 2010. Hedgehog signaling is required at  
390 multiple stages of zebrafish tooth development. *BMC Dev. Biol.* **10**, 119.
- 391 12 Wise, S. B. and Stock, D. W. 2006. Conservation and divergence of *Bmp2a*, *Bmp2b*, and  
392 *Bmp4* expression patterns within and between dentitions of teleost fishes. *Evol. Dev.* **8**,  
393 511–523.
- 394 13 Fraser, G. J., Bloomquist, R. F. and Streelman, J. T. 2008 A periodic pattern  
395 generator for dental diversity. *BMC Biol.* **6**, 32.
- 396 14 Fraser, G. J., Britz, R., Hall, A., Johanson, Z., and Smith, M. M. 2012 Replacing the  
397 first-generation dentition in pufferfish with a unique beak. *Proc. Natl. Acad. Sci.*  
398 *USA* **109**(21), 8179–8184.
- 399 15 Smith, M. M., Okabe, M. and Joss, J. 2009 Spatial and temporal pattern for the  
400 dentition in the Australian lungfish revealed with sonic hedgehog expression

- 401 profile. *Proc. Biol. Sci.* **276**, 623–631.
- 402 16 Buchtova, M., Handrigan, G. R., Tucker, A. S., et al. 2008 Initiation and patterning  
403 of the snake dentition are dependent on Sonic hedgehog signaling. *Dev. Biol.* **319**,  
404 132–145.
- 405 17 Richman, J. M. and Handrigan, G. R. 2011 Reptilian tooth development. *Genesis* **49**,  
406 247–260. (DOI: 10.1002/dvg.20721).
- 407 18 Handrigan, G. R. and Richman, J. M. 2010 Autocrine and paracrine Shh signaling  
408 are necessary for tooth morphogenesis, but not tooth replacement in snakes and  
409 lizards (Squamata). *Dev. Biol.* **337**, 171–186.
- 410 19 Smith, M. M., Fraser, G. J., Chaplin, N., Hobbs, C. and Graham, A. 2009 Reiterative  
411 pattern of sonic hedgehog expression in the catshark dentition reveals a  
412 phylogenetic template for jawed vertebrates. *Proc. Biol. Sci.* **276**, 1225–1233.
- 413 20 Fraser, G. J. and Smith, M. M. 2010 Evolution of development for patterning  
414 vertebrate dentitions: an oro-pharyngeal specific mechanism. *J. Exp. Zool. B Mol.*  
415 *Dev. Evol.* **314B**, 99–112 (DOI: 10.1002/jez.b.21387).
- 416 21 Davis, M. C., Shubin, N. H., and Force, A. 2004 Pectoral fin and girdle development in the  
417 basal actinopterygians *Polyodon spathula* and *Acipenser transmontanus*. *J. Morph.* **262**,  
418 608–628 (DOI: 10.1002/jmor.10264).
- 419 22 Davis, M. C., Dahn, R. D. and Shubin N. H. 2007 An autopodial-like pattern of Hox  
420 expression in the fins of a basal actinoptergian fish. *Nature* **447**, 473–476.
- 421 23 Taylor, W. R. and van Dyke, G. C. 1985 Revised procedures for staining and  
422 clearing small fishes and other vertebrates for bone and cartilage study. *Cybium* **9**,  
423 107–119.
- 424 24 Fraser, G. J., Hulsey, C. D., Bloomquist, R. F., et al. 2009 An ancient gene network  
425 is co-opted for teeth on old and new jaws. *PLoS Biol.* **7**, e31.

- 426 25 Van der Heyden, C. and Huysseune, A. 2000. Dynamics of tooth formation and  
427 replacement in the zebrafish (*Danio rerio*) (Teleostei, Cyprinidae). *Dev. Dyn.* **219**,  
428 486–496.
- 429 26 Tucker, A. S. and Fraser, G. J. 2014. Evolution and developmental diversity of tooth  
430 regeneration. *Semin. Cell Dev. Biol.* 25–26, 71–80 (DOI:  
431 10.1016/j.semcdb.2013.12.013).
- 432 27 Clemen, G., Bartsch, P. and Wacker, K. 1998 Dentition and dentigerous bones in  
433 juveniles and adults of *Polypterus senegalus* (Cladistia, Actinopterygii). *Ann.*  
434 *Anat.* **180**, 211–221.
- 435
- 436

437 **Figure Captions**438 **Figure 1. Expression of *shh*, *bmp4* in *Polyodon spathula* oral and pharyngeal initial**439 **dentitions, stage 41.** (*a-c*, *e*) *shh* expression in tooth buds of cleared whole mount jaws440 compared with (*d*) stage 37 upper jaw, expression restricted to oral surfaces and on first441 infrapharyngobranchial arches. (*a*, *c*) multiple loci on tooth fields of dentary and

442 dermopalatine, only two loci on hypobranchial and palatopterygoid. Arrows indicate

443 alternate timing of strongest expression. (*b*, *e*) strong expression in hypobranchial 1 and

444 palatopterygoid (arrowheads); cone expression in dentary, hypobranchial,

445 dermopalatine, compared to early placode expression on palatopterygoid. (*f-i*) *bmp4*446 expression for comparison to *shh* expression. (*f*, *g*) lower jaw, (*h*, *i*) upper jaw *bmp4* in

447 the dental papillary mesenchyme marks all oral jaw tooth positions. Dental mesenchyme

448 underlies the dental epithelium and expression appears diffuse, however, more intense

449 expression is seen at alternate tooth loci (arrows, *f*, *g*, *i*) with weaker expression450 indicating earlier (older) loci (asterisk), equivalent to *shh* expression pattern.

451 Abbreviations: b1, 2, basibranchials; ba, bone of attachment, cb1-5, ceratobranchials;

452 ch, ceratohyal; de, dentary; d.pal, dermopalatine; hb1, 2, 1st, 2nd hypobranchial; hb1tp,

453 hb2tp, hypobranchial toothplates; hh, hypohyal; hym, hyomandibular; itg, incipient

454 tooth germ; iph, infrapharyngobranchial; iphtp, infrapharyngobranchial toothplate; Mc,

455 Meckel's cartilage; ppt, palatopterygoid; tc, tooth cone; 2ndt, second tooth.

456

457 **Figure 2. Alizarin red, Alcian blue preparations of *Polyodon spathula*, 7dps**458 **showing relative tooth positions.** (*a*, *c*, *g-k*) upper jaw and dorsal pharyngeal skeleton,459 (*b*, *d-f*, *l*) lower jaw and ventral pharyngeal skeleton. (*a*, *b*) chondrocranium and460 branchial arches. (*c*) upper jaw, teeth along dermopalatine bone and separate

461 palatopterygoid tooth plate (lacking membrane bone), with two paired tooth plates

462 caudally (black arrows indicate *j*, *k*). (*d*) lower jaw, ventral pharyngeal skeleton (hyoid,  
 463 1st, 2nd gill arches). (*e*) teeth on dentary bone (arrows, new teeth). (*f*) eight teeth linked  
 464 by bone of attachment on 1st gill arch cartilage (hypobranchial 1), lacking membrane  
 465 bone). (*g*-*i*) left upper jaw, teeth ankylosed to dermopalatine bone, separate  
 466 palatopterygoid tooth plate (arrows, new teeth caudally on dermopalatine (*i*), rostrally  
 467 on palatopterygoid (*h*)). (*h*) palatopterygoid tooth plate, bone of attachment only  
 468 (arrows new teeth). (*j*, *k*) upper jaw tooth plates of (*j*) epibranchial 2, four associated  
 469 teeth, (*k*) hyoid arch, six teeth. (*l*) hypohyal and first two ventral gill arches, with paired  
 470 toothplates, more teeth on hb1 than hb2, more on ventral than dorsal pharyngeal  
 471 toothplates. White arrows=newest unattached teeth. Scale bars *a*, *b*=1mm, *c*-*g*,  
 472 *l*=500um, *h*, *i*=100um; abbreviations as in figure 1.

473

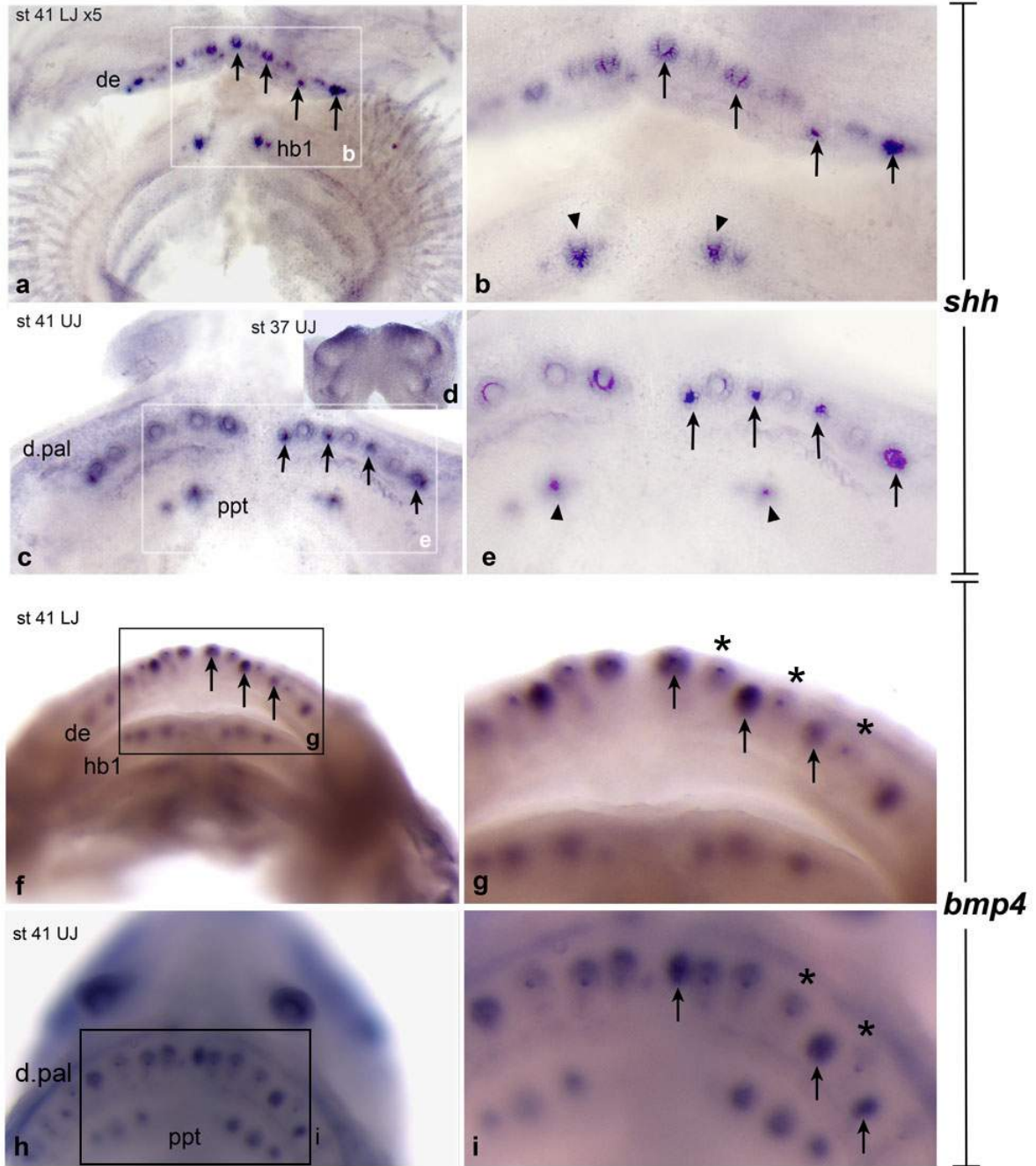
474 **Figure 3. Serial sagittal sections, *Polyodon spathula* (stage 45) after *in situ***  
 475 **hybridisation for *shh* show sequence of tooth morphogenesis.** Photomicrographs,  
 476 low and high magnification (objectives x6.3, x16, x40) of location and rostro-caudal  
 477 timing of *shh* gene expression in all tooth fields relative to tooth germ morphogenesis,  
 478 rostral, left and dorsal, top. (*a-d*) most medial section, expression in dermopalatine  
 479 (cone + collar,  $p^3$ ) and palatopterygoid (placode,  $p^1$ ). (*e*) more lateral section including  
 480 Meckel's cartilage and pharyngeal arches. Expression loci associated with first stages of  
 481 morphogenesis (placode,  $p^1$ ) on the 1st upper branchial arch (iph1), 1st and 2nd  
 482 hypobranchials. By comparison, on 3rd and 4th pharyngeal arches tooth buds foci  
 483 absent, localisation is a field of expression, a stage prior to tooth morphogenesis. (*f*) low  
 484 magnification field of variation in expression loci on dentary and hypobranchial1, with  
 485 collar epithelium downregulated on first tooth (asterisk) and adjacent second tooth germ  
 486 shown as intense expression (arrowhead, weak expression in sensory papilla, arrow as

487 (o, p4). (g) low magnification view of variation in expression at loci on the  
 488 dermopalatine (downregulated) and palatopterygoid strong expression in all dental  
 489 epithelium around dentine cone (late cap stage). (h) tooth cone (tc) developed, and 2nd  
 490 tooth germ (2ndt) at cap stage ( $p^2$ ). (i) 1st hypobranchial, placode stage of *shh*  
 491 expression ( $p^1$ ). (j) tooth cone with second incipient tooth germ (itg), strong expression  
 492 ( $p^4$ ). (k) downregulation from cap to ‘collar’ expression ( $p^3$ ) in 2nd tooth. (l) early tooth  
 493 placode in oral epithelium of 2nd hypobranchial. (m) upper jaw palatoquadrate cartilage  
 494 with tooth germs on dermopalatine and palatopterygoid at different morphogenetic  
 495 stages. (n) four stages of *shh* expression, tooth cone with downregulated expression,  
 496 incipient second tooth germ on dermopalatine, on palatopterygoid, cap stage. (o),  
 497 infrapharyngobranchial (iph1) upregulated strong expression (note evaginated tooth  
 498 germ, placode-cap), alongside weak expression in sensory papilla (arrow). ( $p^{1-4}$ ) four  
 499 stages of *shh* expression in tooth germs, oral epithelium dorsal, contrast enhanced  
 500 (translated into diagram as figure 4 a-d). Scale bars *a, e* = 250um, *b, f, g, m* = 50um, *c,*  
 501 *d, h-l, n-p1-4* = 25um; abbreviations as in figure 1.

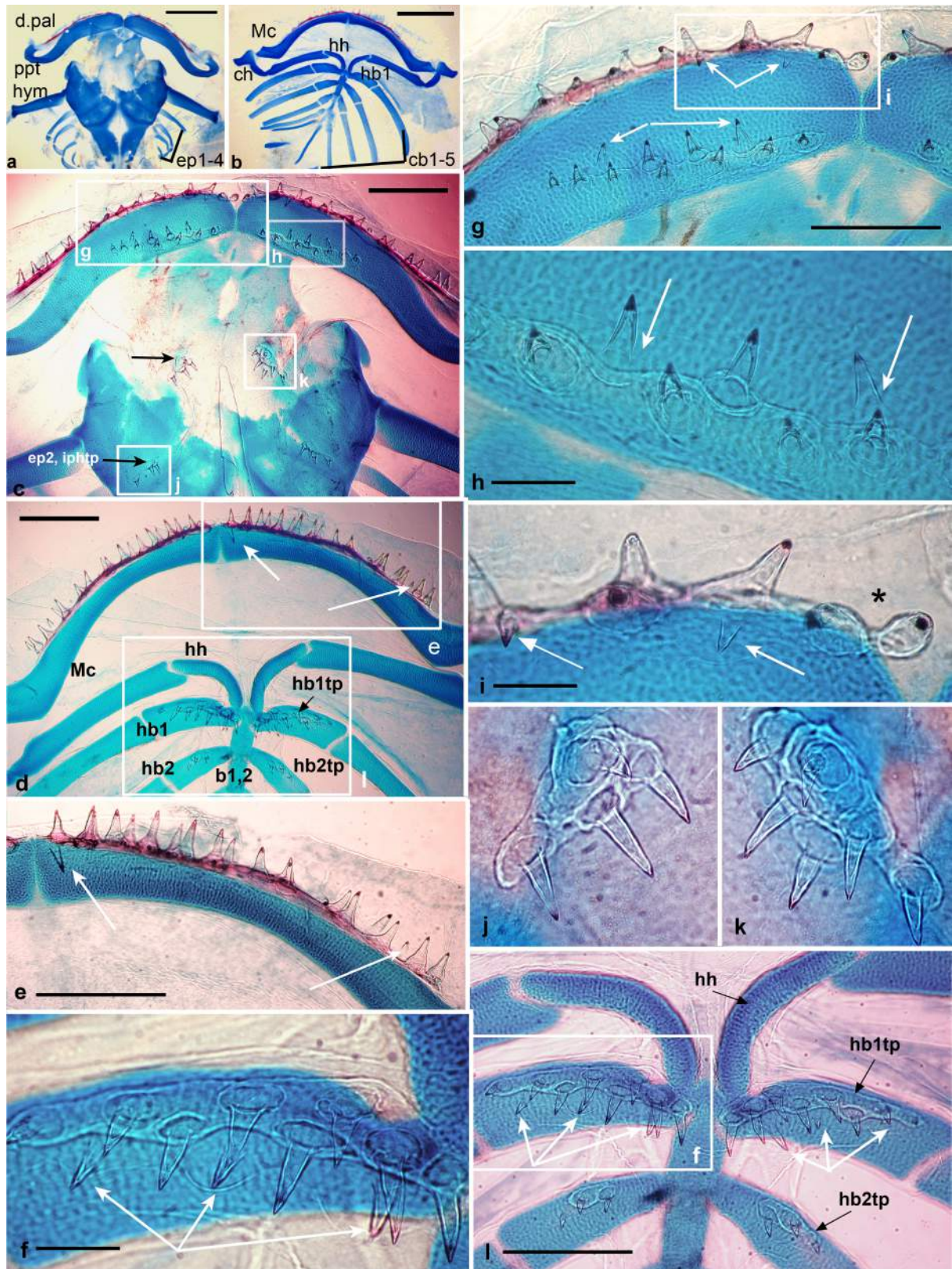
502

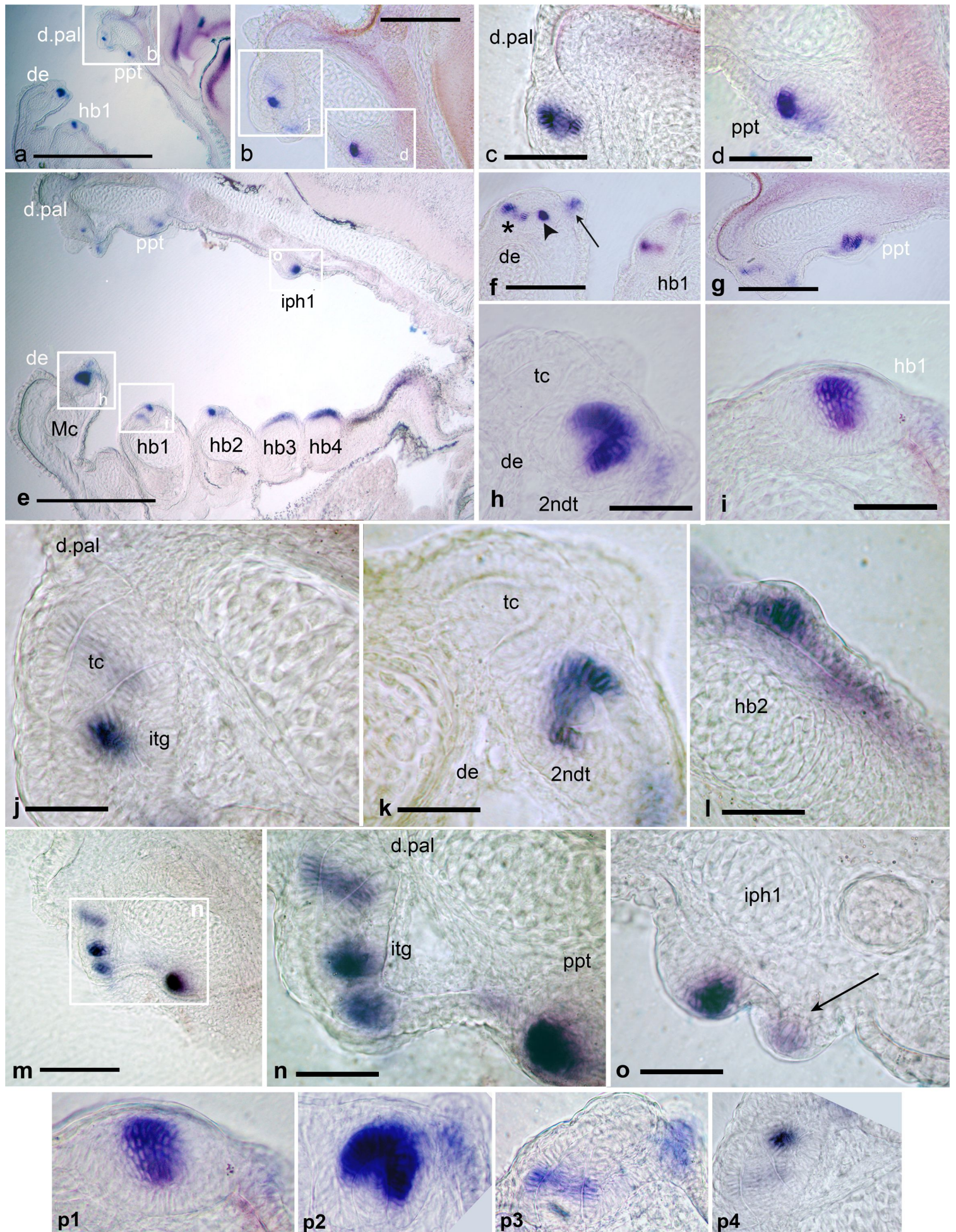
503 **Figure 4.** Diagram summarising stages of tooth germ morphogenesis relative to *shh*  
 504 expression (from figure 3 $p^{1-4}$ ). Intensity of cellular expression is partitioned  
 505 characteristically within the dental epithelium, with negative differentiated, interactive  
 506 cells of dental epithelium shown (proactive d.e.), and also in sensory papilla of taste  
 507 buds on right of tooth germ. (a) cellular partitioning of *shh* expression as ‘placode’  
 508 (localized within epithelium, can be evaginated). (b) ‘cap’, expression in the cap-shaped  
 509 epithelium of tooth germ, surrounding dental papilla. (c) ‘cone+collar’, cones of dentine  
 510 with expression associated with the tooth base, or collar epithelium below the cap. (d)  
 511 ‘cone +bud’, expression in a new site within the outer dental epithelia (incipient bud for

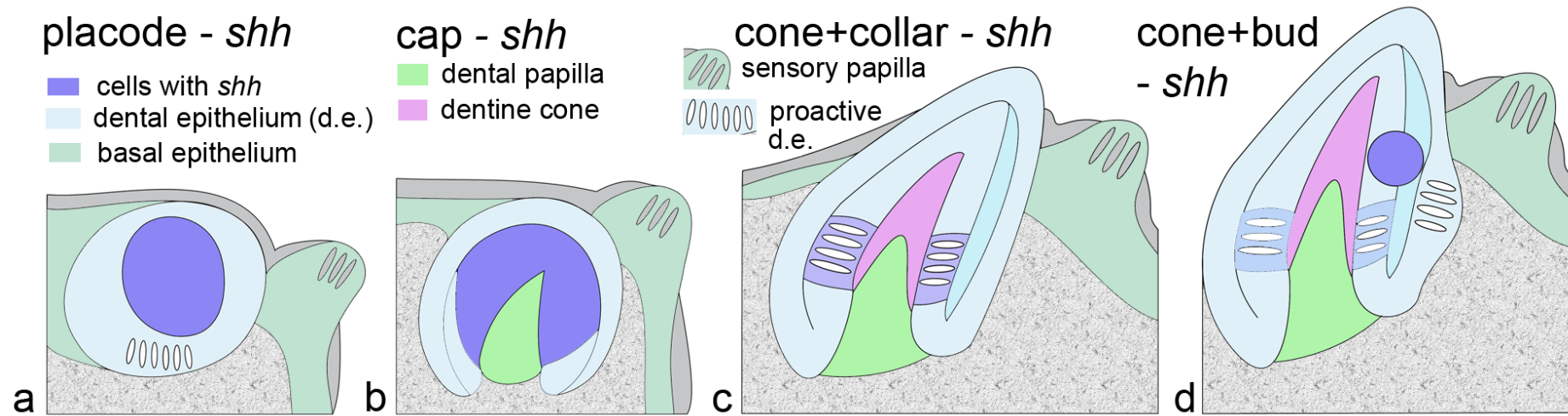
512 new tooth germ).











Specimen	UJ d.pal	UJ ppt	LJ de	UBS iph	UBS epb	LBS hb1	LBS hb2	Figure number
St. 39-40 <i>shh</i>	4+1	0	5	0	0	0	0	ESM 4c-h
St. 41-42 <i>shh</i>	4+2	1+1	7	0	0	1+1	0	1, ESM 4a, i-n
St. 43 <i>shh</i>	8+	2	11+	0	0	1	0	4o, p
Stage 45 <i>shh/bmp</i>	14	8	16-18	2	0	4	0-1	3, ESM 6
<i>7dps larva</i> *	17-20	9-11	21-22	4-6	4	11	3-4	2
<i>TL-345 mm</i> **	55	55	91	0	0	30	10	ESM 1, 2

**Table 1: Rostro-caudal and ventro-dorsal graded trends from oral to pharyngeal sites in tooth addition during development and transition of the embryo to juvenile dentition, *Polyodon spathula*. Differences in total tooth number at each stage of development are shown and reflect a directed pattern in time and space throughout the oro-pharyngeal cavity.** Abbreviations: de, dentary; d.pal, dermopalatine; epb, epibranchial; hb1, 2, hypobranchial 1, 2; iph, infrapharyngobranchial; ppt, pterygopalatine; UBS, LBS, upper, lower branchial skeleton; UJ, LJ, upper, lower jaw. \*Based on n=5 cleared and stained whole mount. \*\*Based on CT scan data. Numbers are per left or right half.